



# Research Project Report

Title: Prediction of pre-critical seismograms from post-critical traces



**Principal Investigator:** Mrinal Sen  
**Co-principal Investigators:** Arthur Weglein and Paul Stoffa

Final report submitted to BP on January 5, 2001

Attention:  
Dr. Scott Mitchell  
[michells@bp.com](mailto:michells@bp.com)  
(281)366-5521

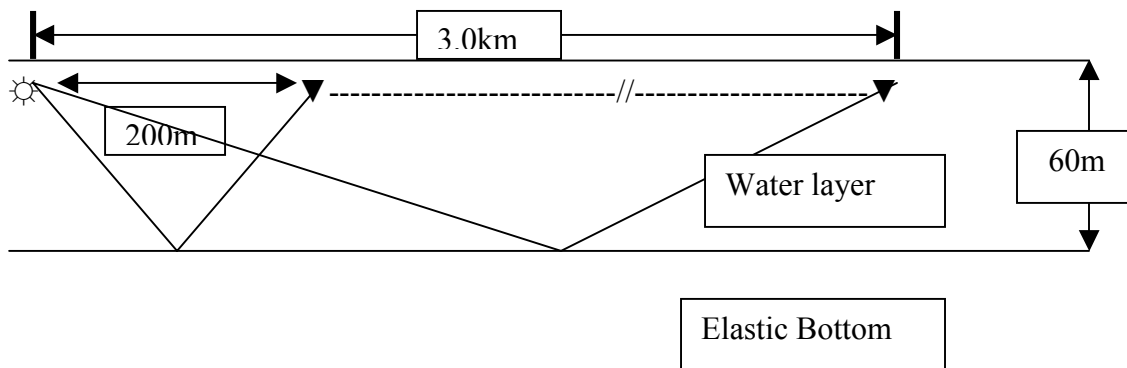
## OBJECTIVE:

The principal objective of this proposal is to study the feasibility of predicting pre-critical seismic traces from the recording of post-critical traces.

## APPROACH:

We carried out numerical experiments with synthetic data to determine if pre-critical traces can be predicted from post-critical traces. We generated synthetic seismograms for three different elastic 1D earth models using a reflectivity approach. We then employed a non-linear seismic waveform inversion approach (based on very fast simulated annealing – VFSA) to derive an earth model, which was then used to predict near-offset traces.

## EXPERIMENTAL GEOMETRY:



The experimental geometry is shown in the above figure; a streamer is towed in a region where the water depth is 60m (Two way time = 80 ms).

The first receiver offset = 200m,

Receiver spacing = 20m, and

Maximum source-receiver offset = 3.0 km.

Note that the take-off angle corresponding to the first primary reflection at the nearest receiver =  $\text{atan}(100/60) = 59^\circ$ . This corresponds to a ray-parameter = 0.57 sec/km.

## FORWARD MODELING:

Our forward modeling technique is based on a reflectivity algorithm described in detail by Kennett (1984). In a reflectivity approach, the equation of motion and the constitutive relations are transformed into frequency-wavenumber (ray-parameter) domain resulting in a first order system of ordinary differential equation (ODE) in depth ( $z$ ). The first order ODE is then solved by using Kennett's reflection matrix approach in the frequency-ray parameter ( $\omega, p$ ) domain. Four reflection and transmission matrices are computed for each layer with an interface and the composite response is evaluated using Kennett's iteration

equation. The final response in the offset-time domain is computed by plane wave transformation of the data in the frequency-wavenumber domain. Intermediate results in the delay time – ray-parameter ( $\tau$ -p) domain can be obtained simply by inverse temporal Fourier transformation.

### **SOURCE WAVELET:**

We used a Ricker wavelet with a peak frequency of 40 Hz in all our applications to generate synthetic pressure response for the experimental geometry shown in the figure.

### **OPTIMIZATION/WAVEFORM INVERSION:**

The details of the seismic waveform inversion are described in chapter 6 of Sen and Stoffa (1995). In a seismic waveform inversion, synthetic seismograms for an assumed earth model are compared with the recorded seismograms. If the match is not adequate, the model is perturbed until the fit is acceptable. Optimization methods are employed to update the model and to find an optimal model. The salient features of our approach are as follows:

- We use plane wave transformed data since forward modeling in this domain is extremely efficient,
- We use a global optimization method called very fast simulated annealing (VFSA) for model update and to find an optimal model,
- We use a normalized cross-correlation function that is sensitive to both amplitude and phase, as the objective function, and
- We carry out our search in a user-supplied search window enabling us to speed up the computation and restrict our search to realistic values of earth model parameters.

## **NUMERICAL EXPERIMENTS**

### MODEL I: Soft Bottom

The elastic parameters for this model are as follows:

$$V_p = 1.7 \text{ km/sec,}$$

$$V_s = 0.8 \text{ km/sec,}$$

and

$$\text{Density} = 1.3 \text{ gm/cc.}$$

Synthetic (x,t) gathers in the offset range of 0.2-3.0 km are shown in Fig 1. Realistic anelastic attenuation values were used in generating the synthetic seismograms. The data contain primary sea-floor reflections and several of its multiples along with the head waves. For this model, the critical angle is  $61.9^\circ$ , which corresponds to a ray-parameter of 0.588 sec/km. Thus we notice that we have pre-critical primary reflection only in the range of  $59^\circ$  to  $61.9^\circ$ , i.e., a ray-parameter range of 0.57 sec/km to 0.588 sec/km. All

other primary reflection arrivals are post-critical arrivals. The (x,t) gathers shown in Fig 1 were used to generate ( $\tau$ -p) gathers in the ray-parameter range of 0.57 to 0.66 sec/km using a true-amplitude frequency-domain plane-wave transformation code. The primaries and all the multiples are clearly visible (Fig 2a). The search window used in the VFSA inversion is given below:

	Vpmin	Vpmax	Vsmin	Vsmax	Rhomin	Rhomax	TWT_min	TWT_max
Layer 1	1.5	1.5	0.0	0.0	1.0	1.0	0.72	0.88
Layer 2	1.3	2.2	0.6	1.4	1.0	1.8	-	-

TWT : Two-way-time

The best-fit model obtained by VFSA (dashed line) is compared with the true model in Fig. 2(b).

We then computed seismograms in the offset range of 20m to 200m using the true and the reconstructed models. The difference between the two sets of seismograms is negligible (Fig. 3 right panel).

#### MODEL 2: Hard Bottom

The elastic parameters for this model are as follows:

Vp = 2.0 km/sec,  
Vs = 0.8 km/sec,  
and  
Density = 1.4 gm/cc.

Synthetic (x,t) gathers in the offset range of 0.2-3.0km are shown in Fig 4. The data contain primary sea-floor reflections and several of its multiples along with the head waves. For this model, the critical angle is  $48.6^\circ$ , which corresponds to a ray-parameter of 0.5 sec/km. Thus we record only the post-critical reflections the ray-parameter range of 0.57 sec/km to 0.588 sec/km. The (x,t) gathers shown in Fig 4 were used to generate ( $\tau$ -p) gathers in the ray-parameter range of 0.57 to 0.66 sec/km using a true-amplitude frequency-domain plane-wave transformation code. The primaries and all the multiples are clearly visible (Fig 5a). The search window used in the VFSA inversion is given below:

	Vpmin	Vpmax	Vsmin	Vsmax	Rhomin	Rhomax	Twt_min	Twt_max
Layer 1	1.5	1.5	0.0	0.0	1.0	1.0	0.72	0.88
Layer 2	1.3	2.5	0.6	1.4	1.0	1.8	-	-

The best-fit model obtained by VFSA (dashed line) is compared with the true model in Fig. 5(b).

We then computed seismograms in the offset range of 20m to 200m using the true and the reconstructed models. The difference between the two sets of seismograms is small (Fig. 6 right panel).

Next we added a small amount of (1%) random noise to the data shown in Fig 4 (Figure 7) and obtained ( $\tau$ -p) gathers shown in Fig 8(a). The noisy ( $\tau$ -p) data were then used in the waveform inversion; all other parameters were the same as those in the noise-free case. The results are shown in Figure 8(b) and the data predictions are shown in Fig. 9.

### MODEL 3: Multi-layered Case

The elastic parameters of the model are given below:

Layer No.	Vp	Vs	Rho	TWT
1	1.5	0.0	1.0	0.08
2	1.7	0.7	1.3	0.18
3	1.85	0.9	1.4	0.28
4	1.95	1.1	1.5	0.38
5	2.10	1.3	1.7	-

Synthetic (x,t) gathers in the offset range of 0.2-3.0 km are shown in Fig 10. The data contain primary sea-floor and subsurface reflections and several of their multiples along with the head waves. For this model, the critical angle for the sea-floor primary is  $61.9^\circ$ , which corresponds to a ray-parameter of 0.588 sec/km. Thus we record sea-floor pre-critical reflections in the ray-parameter range of 0.57 sec/km to 0.588 sec/km. The (x,t) gathers shown in Fig 10 were used to generate ( $\tau$ -p) gathers in the ray-parameter range of 0.49 to 0.66 sec/km using a true-amplitude frequency-domain plane-wave transformation code. The primaries and all the multiples are clearly visible (Fig 11a). Note that the sea-floor primaries in the range of 0.49-0.57 sec/km are not recorded in the offset range for this experiment. In the ( $\tau$ -p) data, the sea-floor primaries in this range are transform artifacts (leakage) that can be considered noise. The search window used in the VFSA inversion is given below:

	Vpmin	Vpmax	Vsmin	Vsmax	Rhomin	Rhomax	Twt_min	Twt_max
Layer 1	1.5	1.5	0.0	0.0	1.0	1.0	0.72	0.88
Layer 2	1.3	1.9	0.5	0.9	1.0	1.5	0.16	0.20
Layer 3	1.5	2.0	0.7	1.1	1.2	1.6	0.26	0.30
Layer 4	1.8	2.2	0.9	1.3	1.3	1.7	0.36	0.40

Layer 5	1.8	2.3	1.1	1.5	1.5	1.9	-	-
---------	-----	-----	-----	-----	-----	-----	---	---

The best-fit model obtained by VFSA (dashed line) is compared with the true model in Fig. 11(b).

We then computed seismograms in the offset range of 20m to 200m using the true and the reconstructed models. The difference between the two sets of seismograms is negligible (Fig. 12 right panel).

## SUMMARY

We generated reflectivity synthetic seismograms in the offset range 0.2-3.0 km for a shallow water experiment for a series of subsurface models. These were then used in a nonlinear VFSA inversion to predict earth models, which were then used to generate seismograms in the near-offset regions. Our experiments showed that in all of our experiments, we were able to predict the near-offset data reasonably well. Note that given the post-critical data alone, the inverse problem has non-unique solutions. In all cases, we made several inversion runs with different random starting models (within the search window) and obtained multiple solutions that are slightly different but have the same level of data misfit. In this report, we only showed one of the many models. Even with the broad search window used in all the inversion runs, we were able to obtain models that range within small values of the model parameters. In all cases the data prediction appears acceptable. Whether such data prediction is adequate for multiple attenuation can only be assessed with further studies using field data.

Here we outline the following limitations of our approach. We assumed that

- The source-time function or the wavelet and the source and receiver depths are known exactly,
- In the multi-layered inversion (Model 3) we assumed prior knowledge of the number of subsurface reflectors,
- Direct waves were not included in the modeling and inversion (Arthur Weglein and one of his students are developing a robust algorithm for direct wave removal which can be used in pre-processing of field data),
- The subsurface attenuation structure was assumed known.

These limitations and deviation from 1D earth structure can cause potential errors in the real data inversion. Such problems should be addressed in a future study (possible second phase of the project) with application to real data. Nonetheless the results from using a very small range of ray-parameter are highly encouraging..

**REFERENCE:**

Kennett, B. L. N., 1984, Seismic wave propagation in stratified media, The Cambridge University Press.

Sen, M. K., and P. L. Stoffa, 1995, Global optimization methods in geophysical inversion, Elsevier Science Publishing Company, The Netherlands.

# SOFT BOTTOM

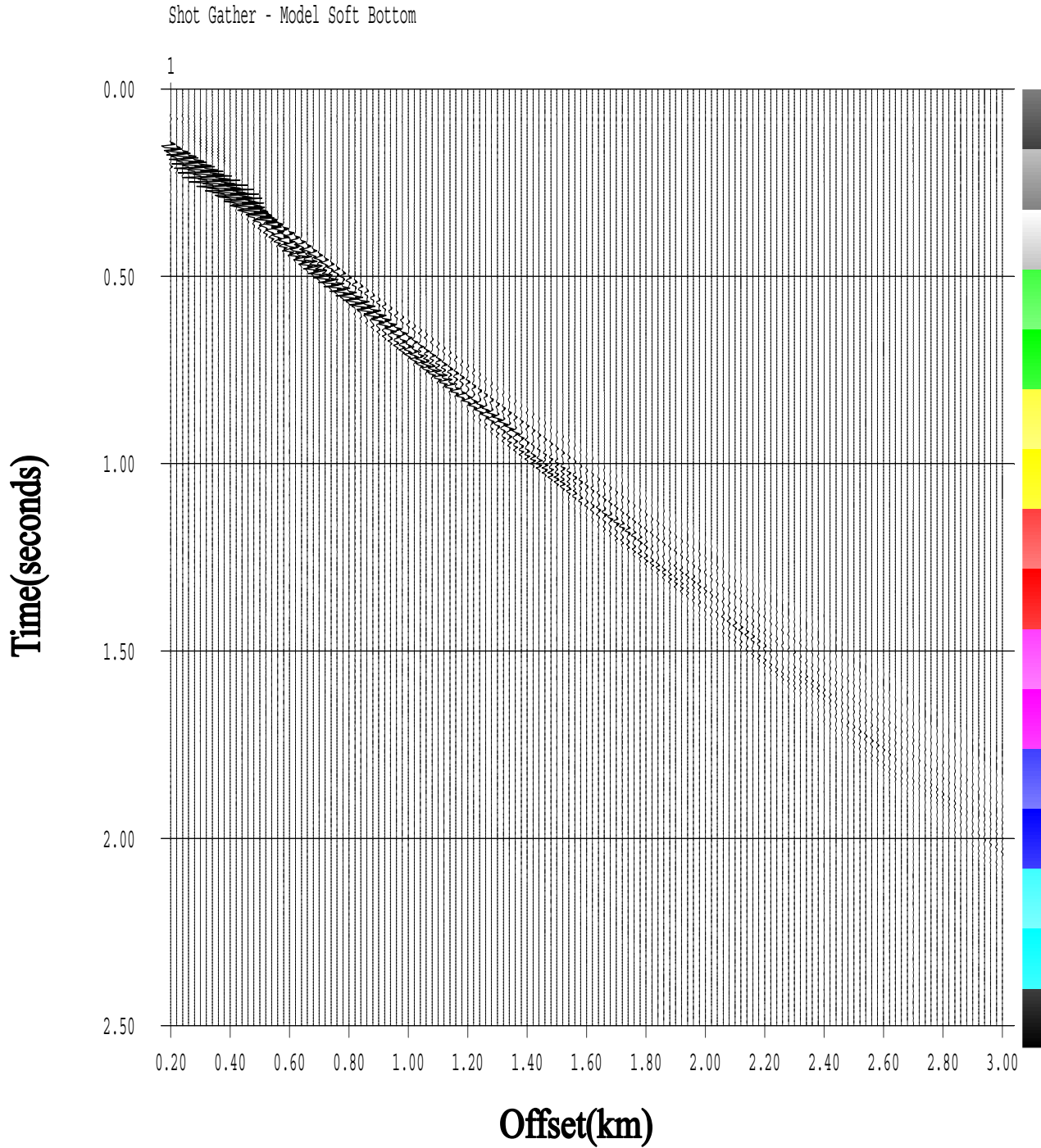


Figure 1. Synthetic seismograms for a water layer over half-space (soft) model computed by using a full waveform modeling algorithm: Water layer reverberations and head waves are clearly visible.



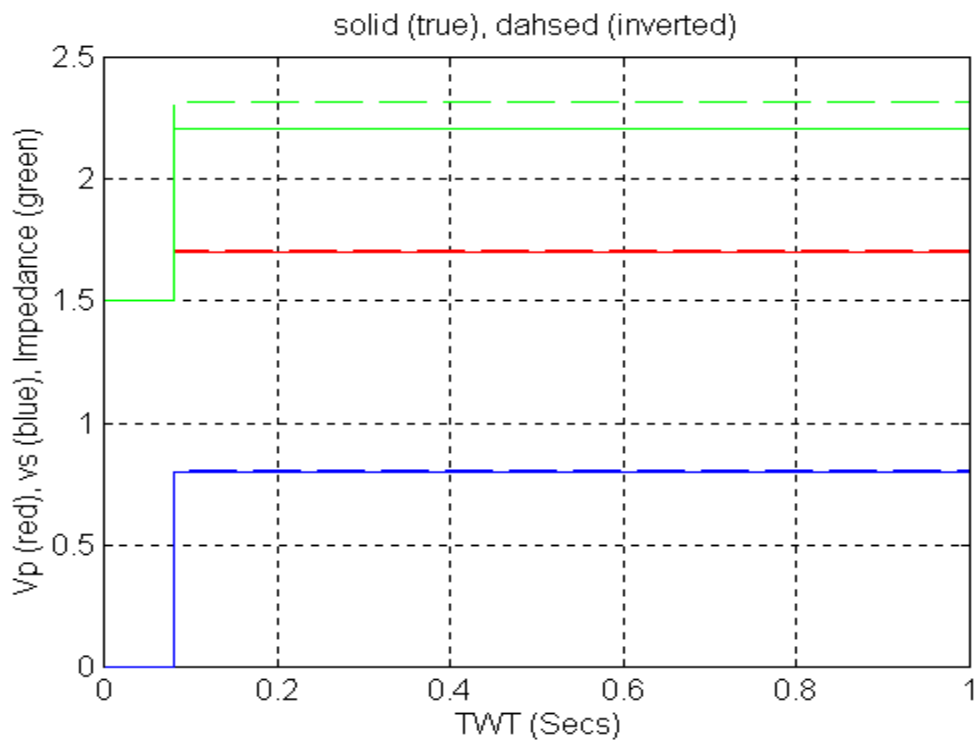
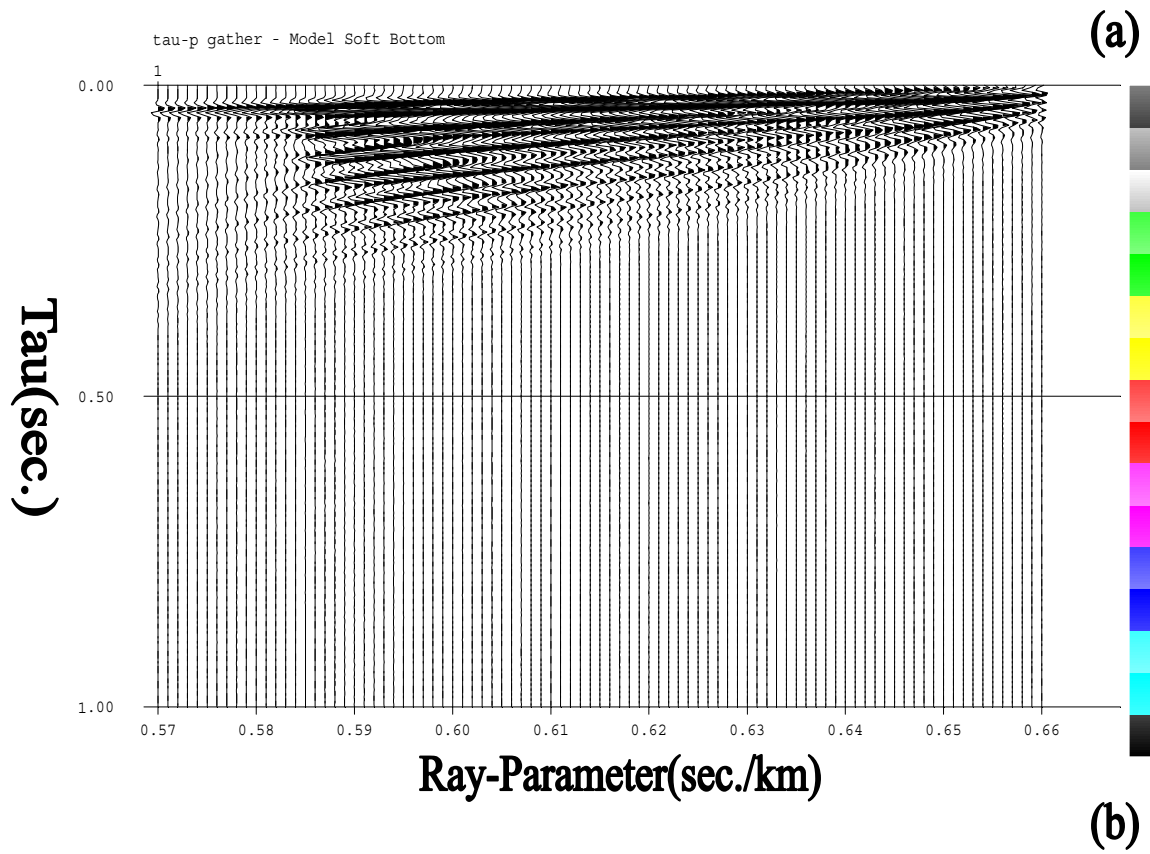


Figure 2: (a) tau-p seismograms generated by a true-amplitude plane wave transformation of the data shown in Fig. 1: these data were used in a non-linear full waveform inversion. (b) inversion result: The true and reconstructed  $V_p$ ,  $V_s$ , and impedance models.

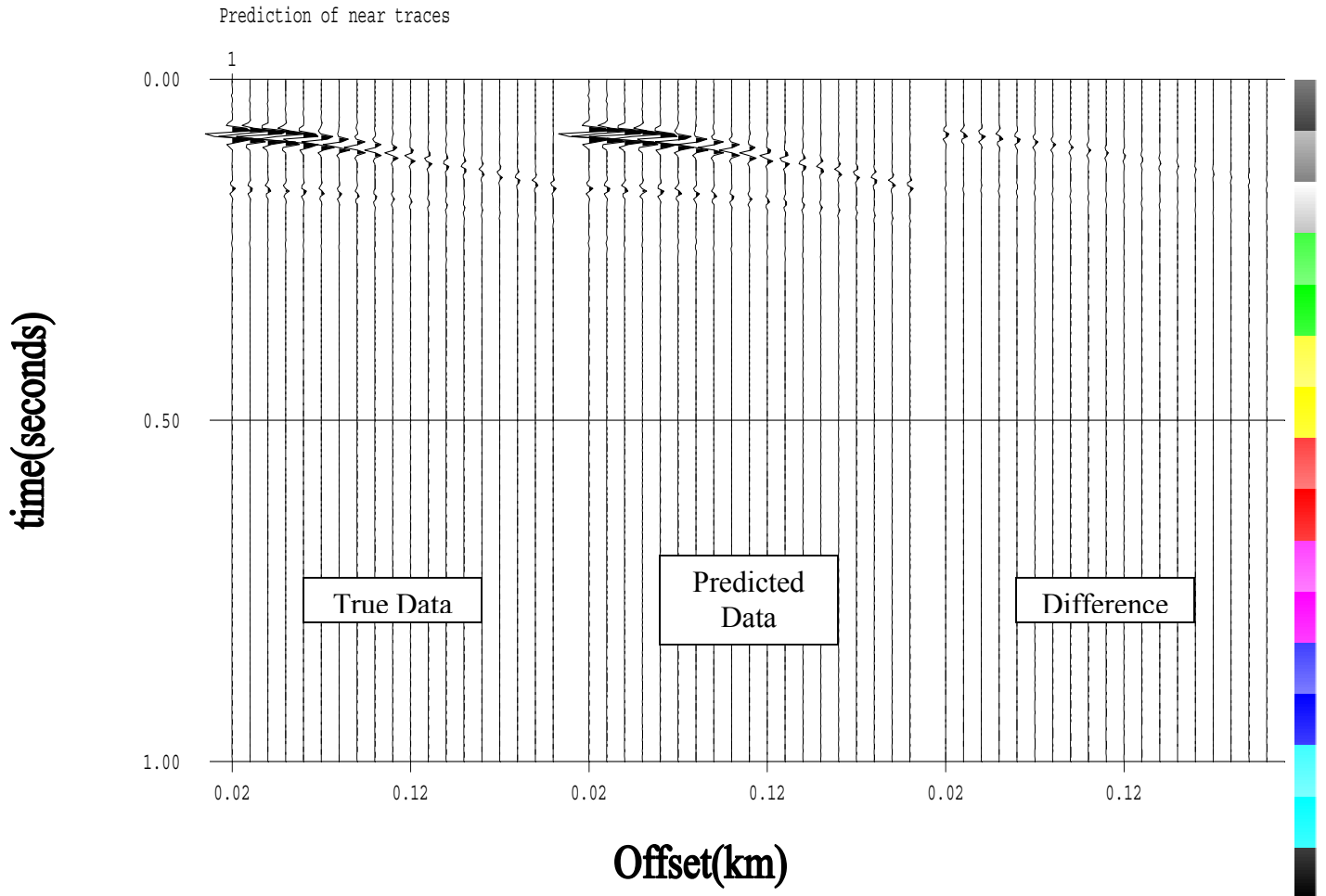


Figure 3: Data Prediction: The near traces predicted by the reconstructed model (middle panel) are compared with those for the true model (left panel). The difference (right panel) between the two sets is very small.

# HARD BOTTOM – NOISE FREE CASE

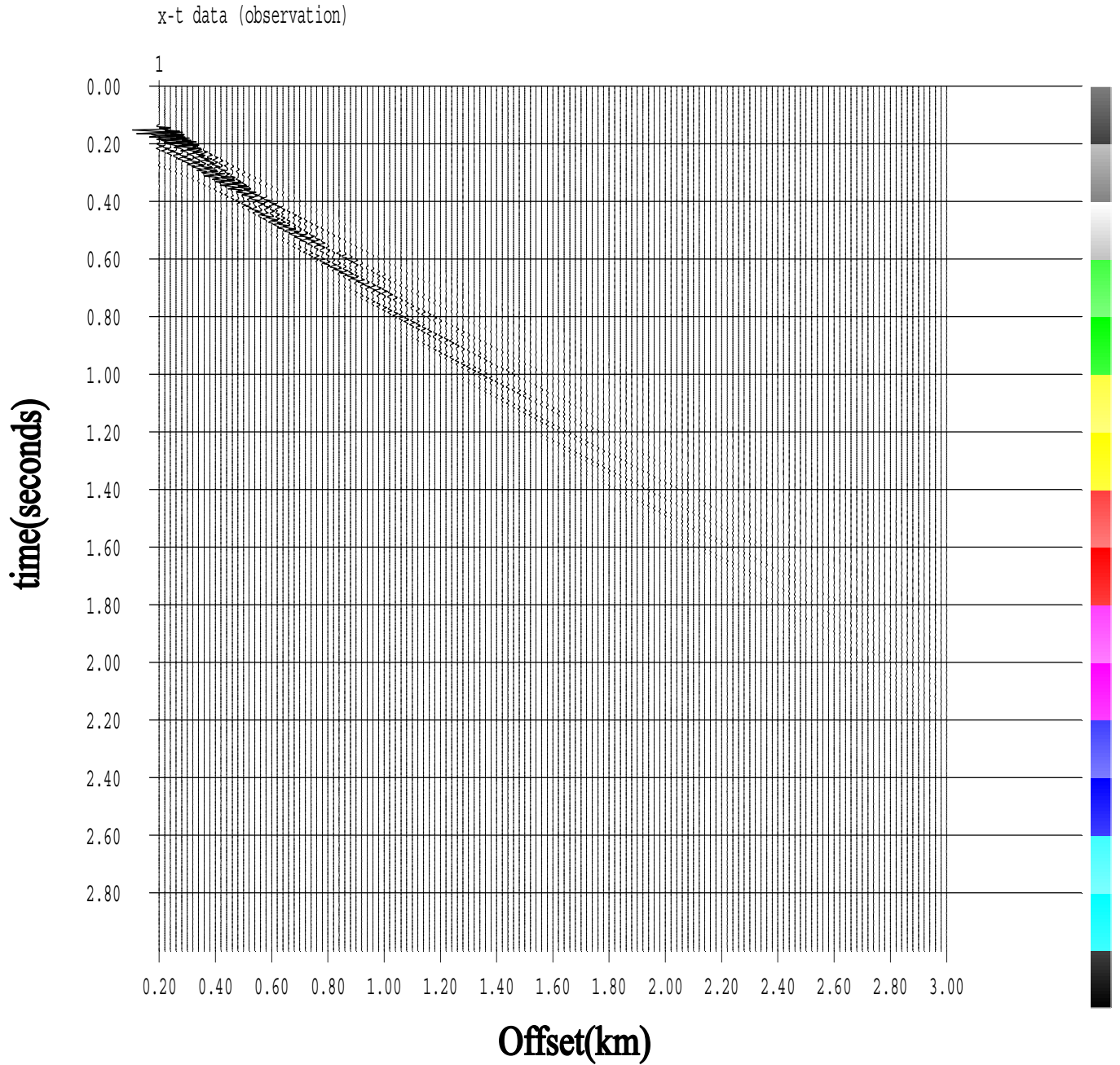


Figure 4. Synthetic seismograms for a water layer over half-space (hard bottom) model computed by using a full waveform modeling algorithm: Water layer reverberations and head waves are clearly visible. Notice that in the offset range (0.2-3.0 km), only the post-critical arrivals are recorded.

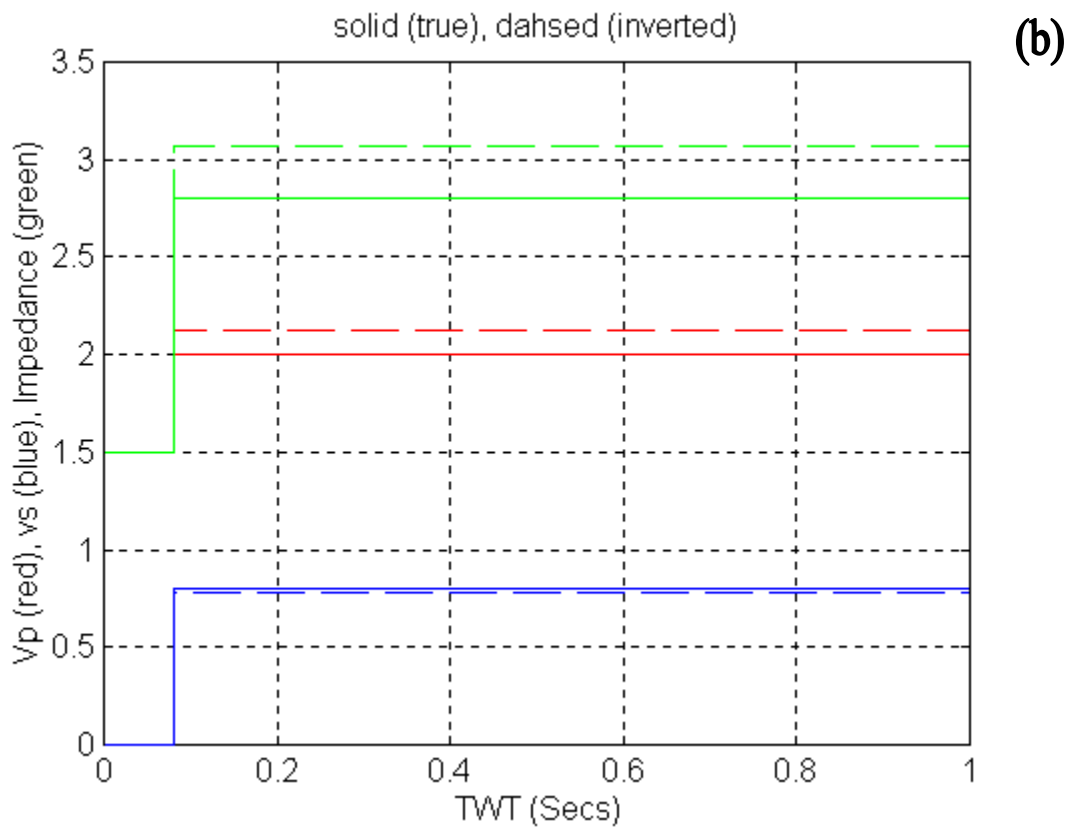
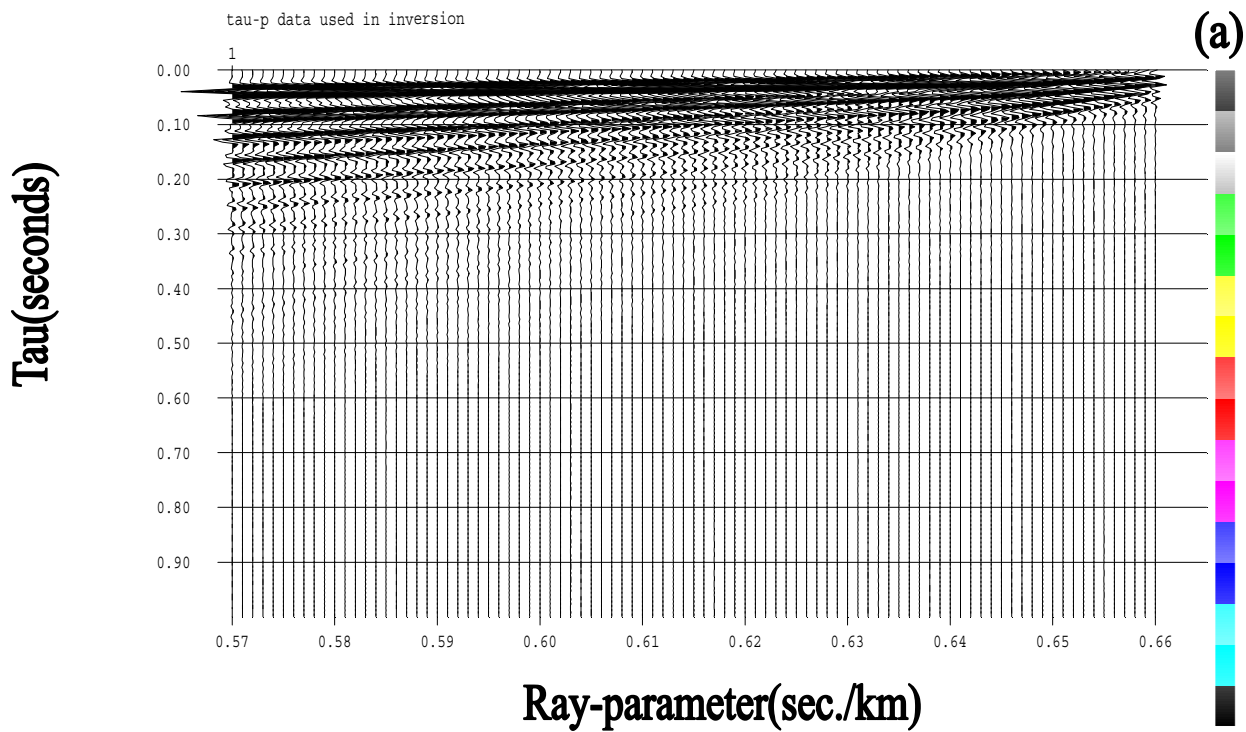


Figure 5: (a) tau-p seismograms generated by a true-amplitude plane wave transformation of the data shown in Fig. 4: these data were used in a non-linear full waveform inversion. (b) inversion result: The true and reconstructed Vp, Vs, and impedance models.

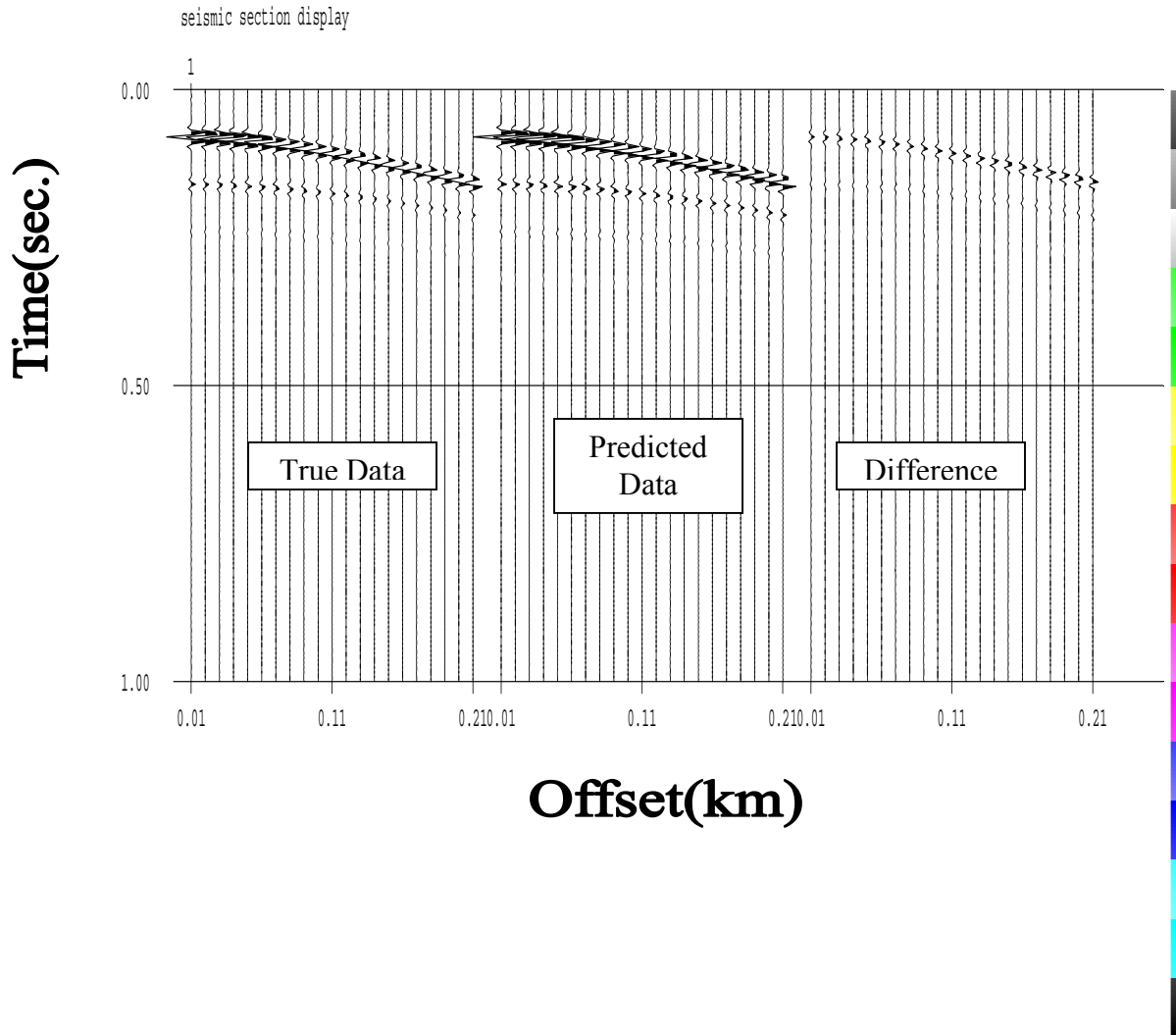


Figure 6: Data Prediction: The near traces predicted by the reconstructed model (middle panel) are compared with those for the true model (left panel). The difference (right panel) between the two sets is small.

## Hard Bottom with Noise

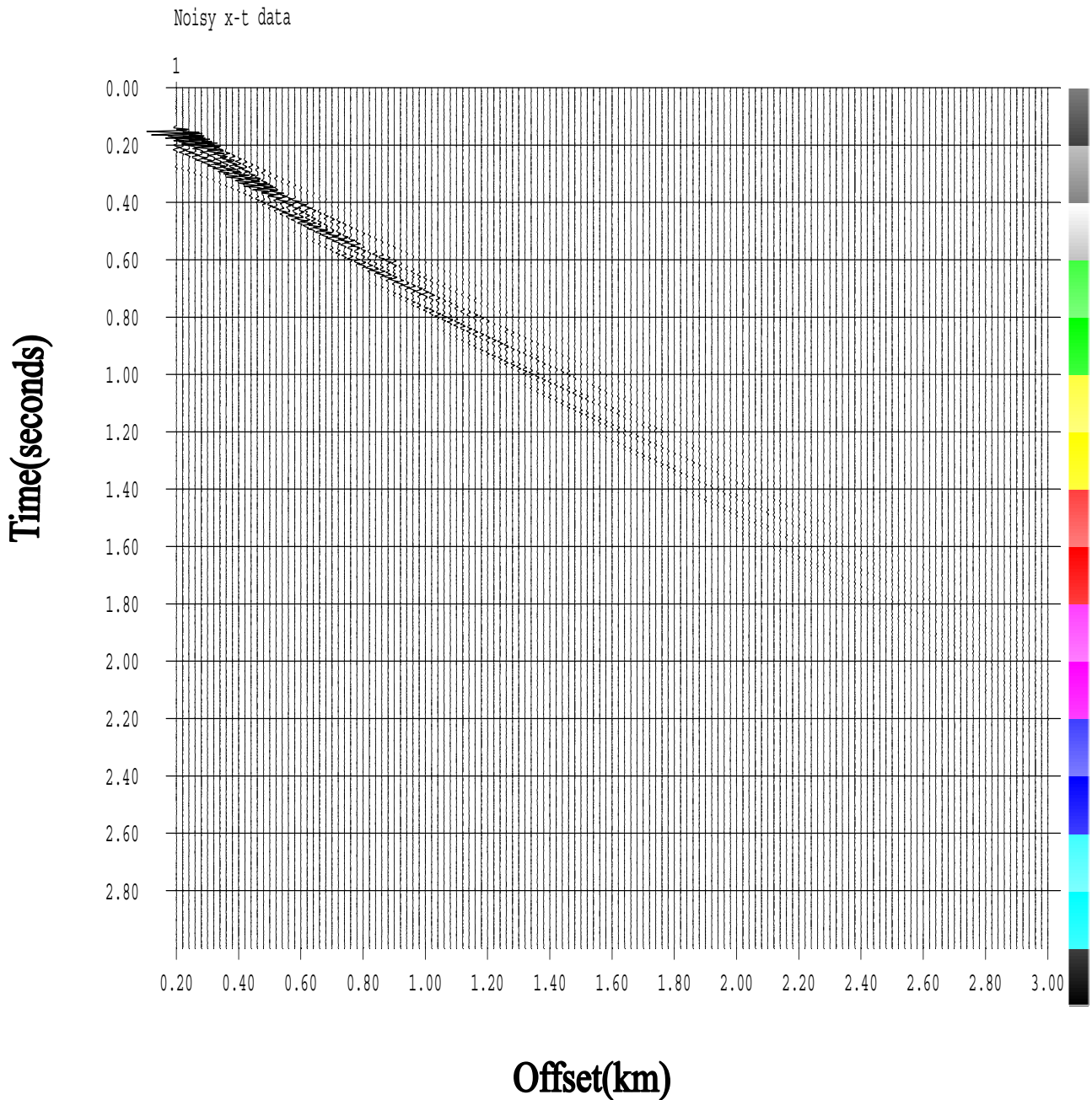


Figure 7. Synthetic seismograms for a water layer over half-space (hard bottom) model computed by using a full waveform modeling algorithm: Water layer reverberations and head waves are clearly visible. Notice that in the offset range (0.2-3.0 km), only the post-critical arrivals are recorded. These data are the same as those shown in fig. 4 with random noise added to them.

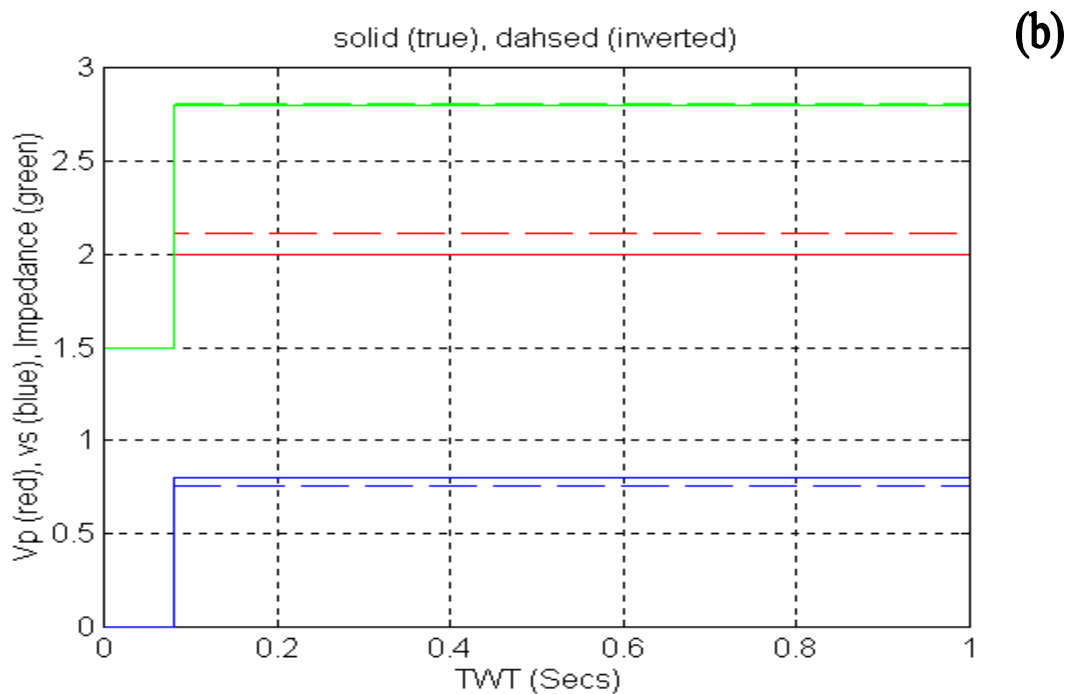
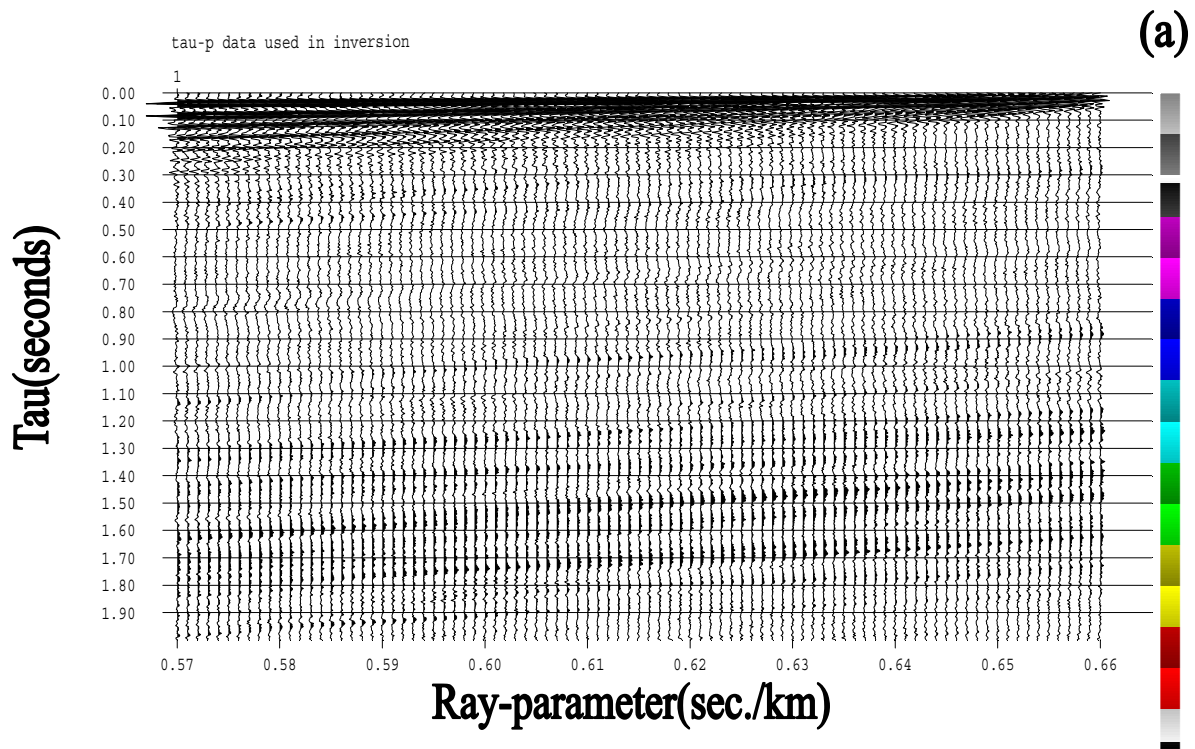


Figure 8: (a) tau-p seismograms generated by a true-amplitude plane wave transformation of the data shown in Fig. 7: these data were used in a non-linear full waveform inversion. (b) inversion result: The true and reconstructed  $V_p$ ,  $V_s$ , and impedance models.



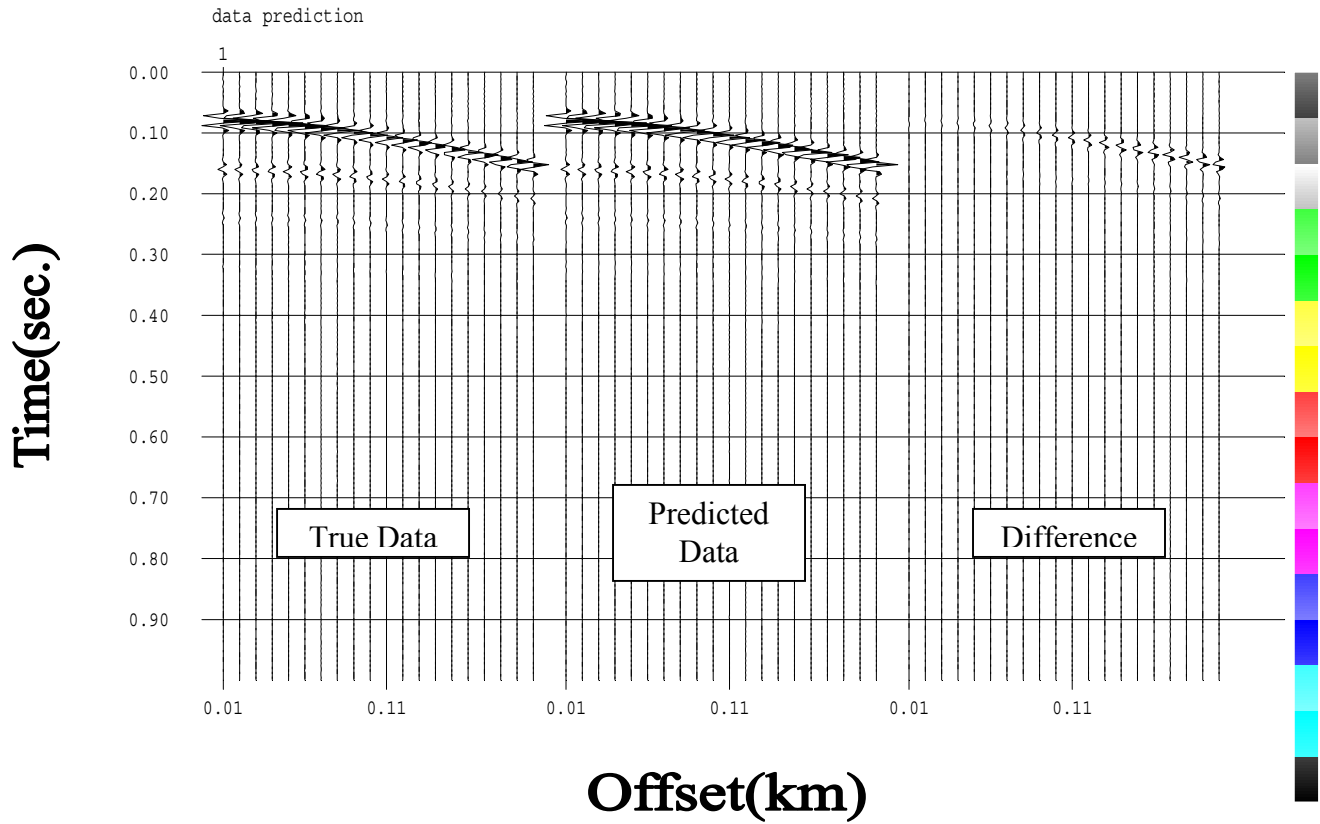


Figure 9: Data Prediction: The near traces predicted by the reconstructed model (middle panel) are compared with those for the true model (left panel). The difference (right panel) between the two sets is very small.



## Multi\_layer Case

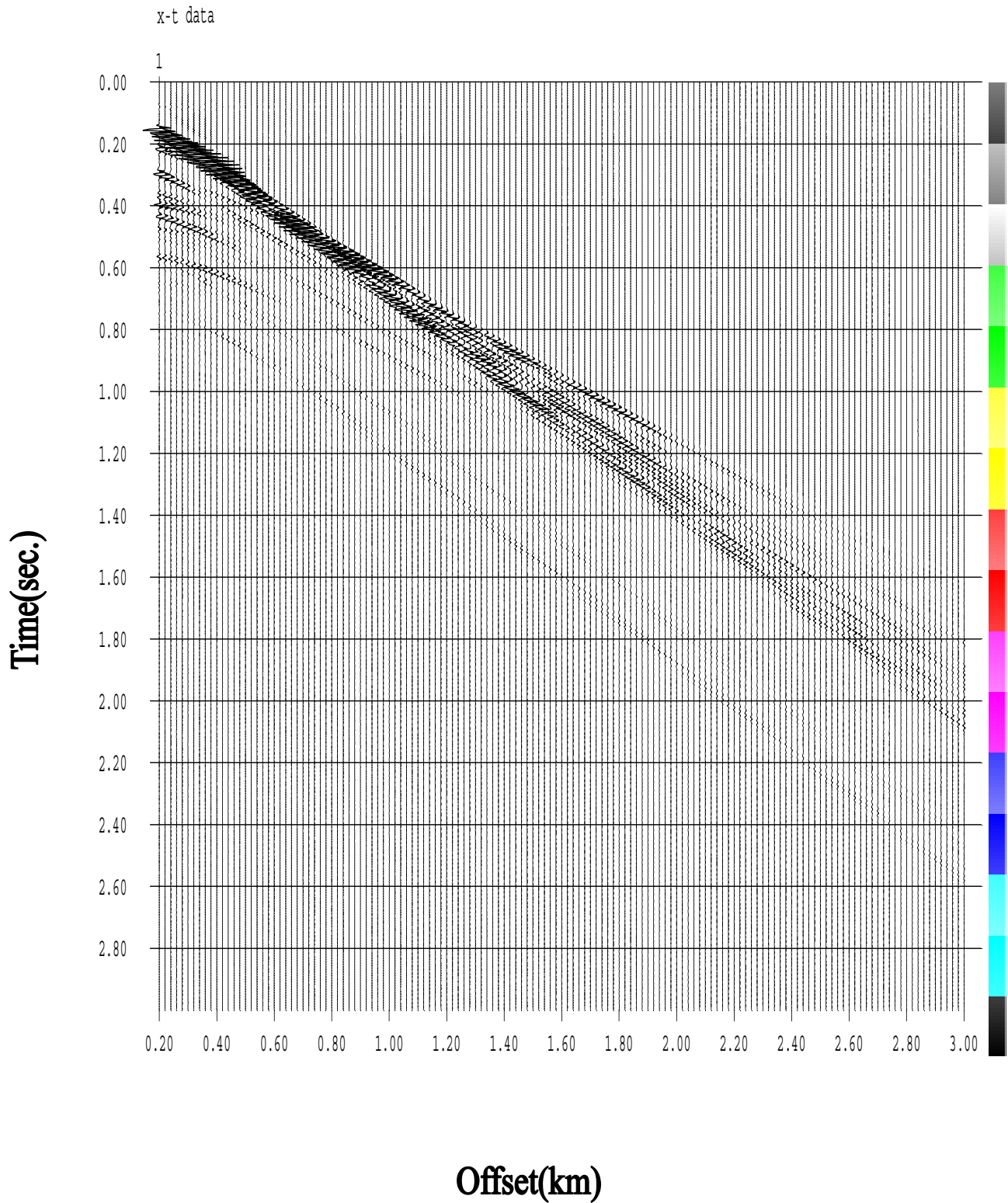


Figure 10. Synthetic seismograms for a water layer over multi-layered half-space (soft bottom) model computed by using a full waveform modeling algorithm: Water layer reverberations and head waves are clearly visible..

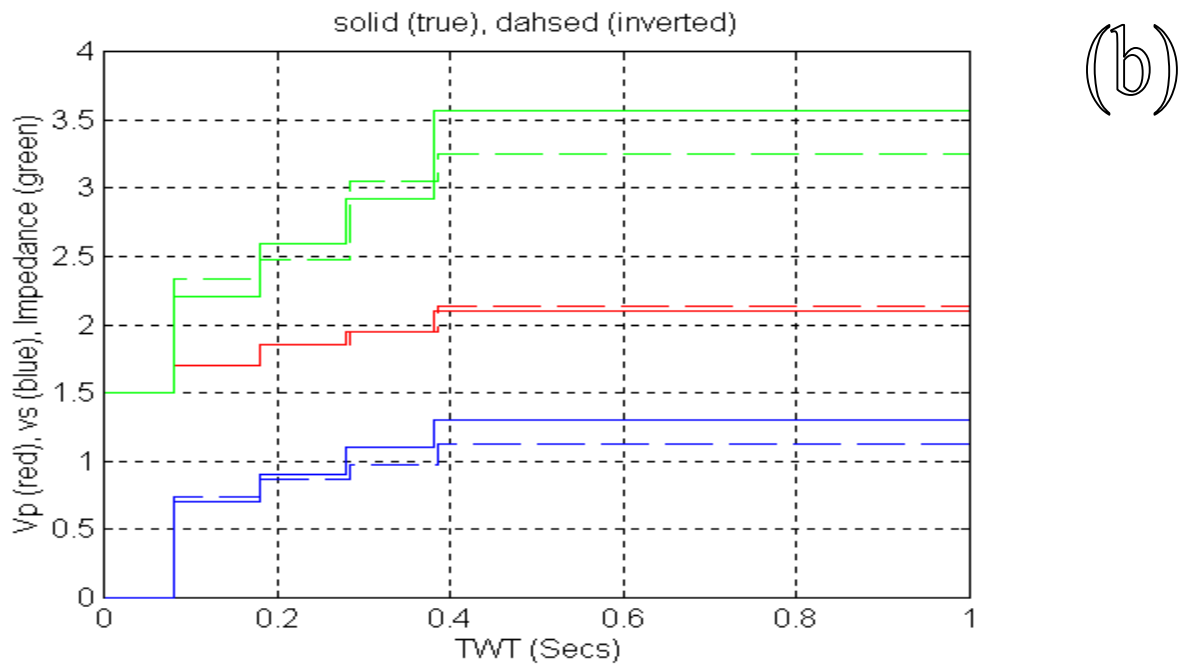
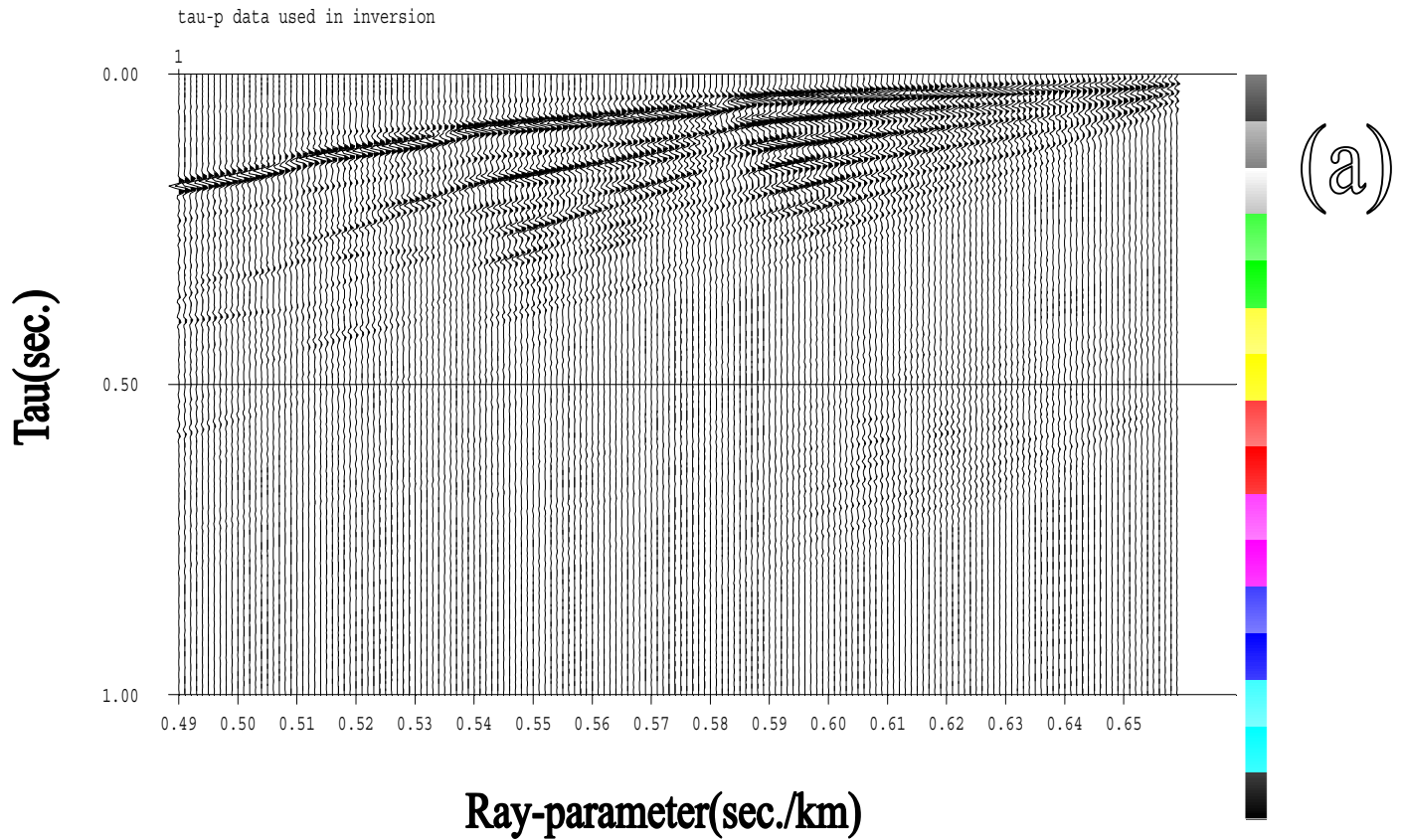


Figure 11: (a) tau-p seismograms generated by a true-amplitude plane wave transformation of the data shown in Fig. 10: these data were used in a non-linear full waveform inversion. (b) inversion result: The true and reconstructed Vp, Vs, and impedance models.

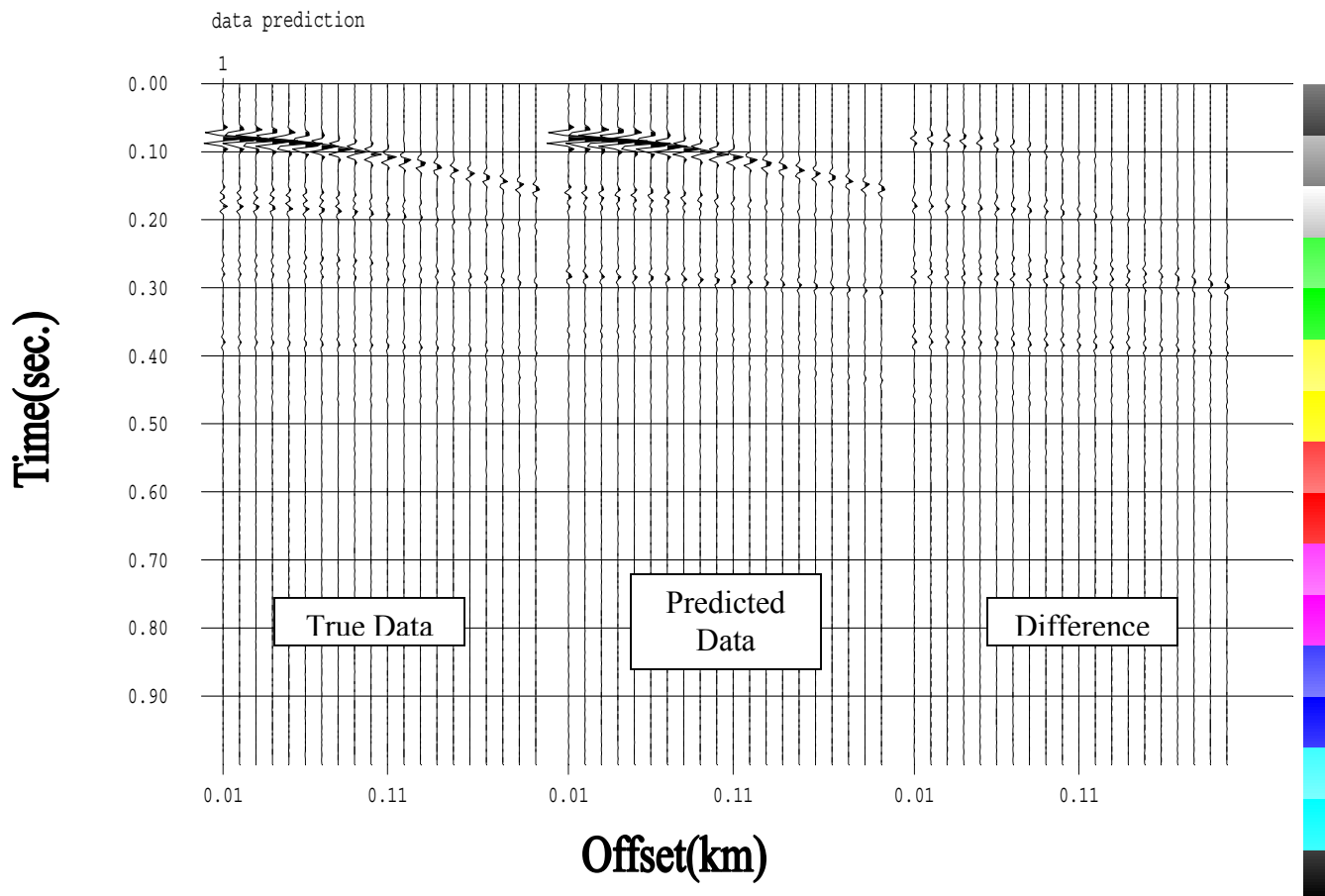


Figure 12: Data Prediction: The near traces predicted by the reconstructed model (middle panel) are compared with those for the true model (left panel). The difference (right panel) between the two sets is very small.